

**Supporting information for**

***Atomic layer deposition of Pd nanoparticles and single atoms on  
self-supported carbon monolithic catalysts synergistically boost  
hydrogen evolution reaction***

Bin Zhang, Xulong Song, Zhiheng Wang, Binbin Xu, Tuo Ji, Lilong Zhang, Xiaohua Lu, and

Jiahua Zhu\*

State key Laboratory of Materials-oriented Chemical Engineering, College of Chemical  
Engineering, Nanjing Tech University, Nanjing 211816, China

\*Corresponding author. J.Z. E-mail: jhzhu@njtech.edu.cn

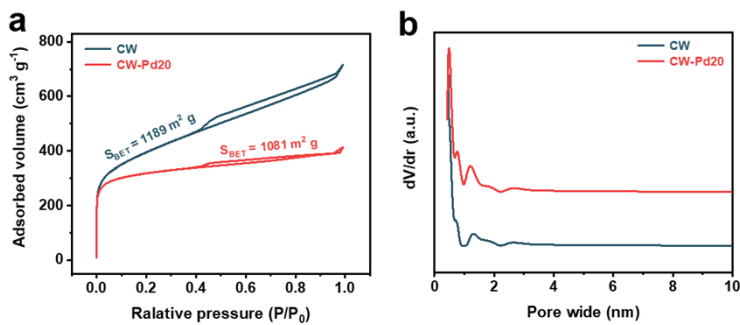


**Figure S1.** (a)  $\text{N}_2$  adsorption/desorption isotherms and (b) pore size distribution of CW and CW-Pd20.

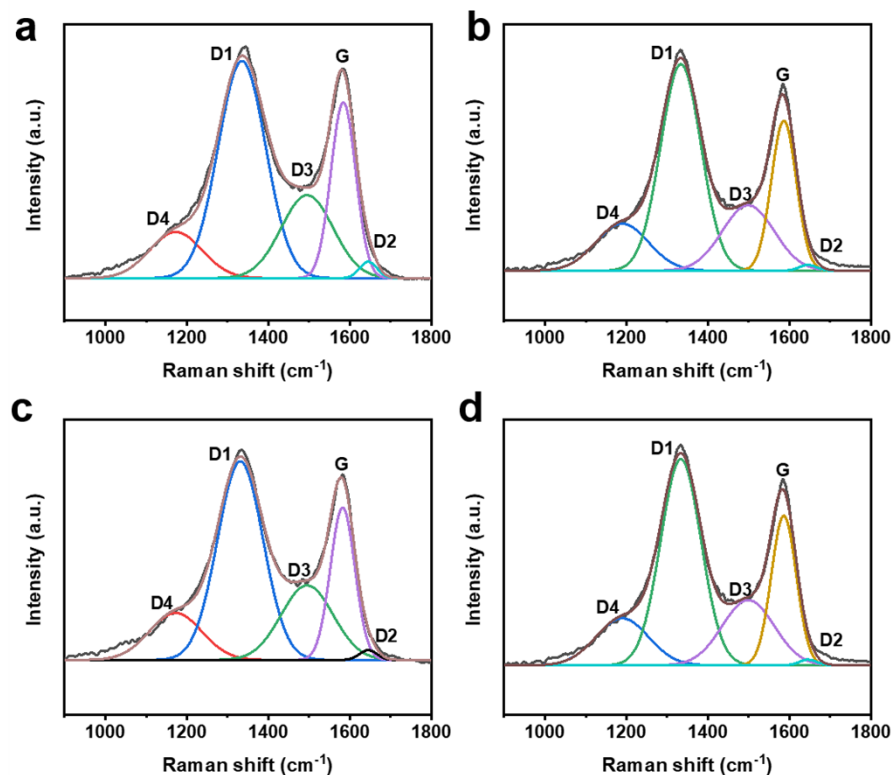


**Figure S2.** Raman spectra deconvolution results of a) CW, b) CW-Pd10, c) CW-Pd20, d) CW-Pd30.

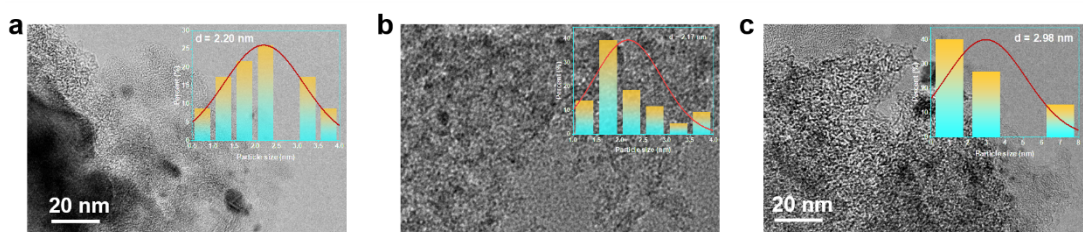


**Figure S3.** TEM images and size distribution (inset) of a) CW-Pd10, b) CW-Pd20, c) CW-Pd30.

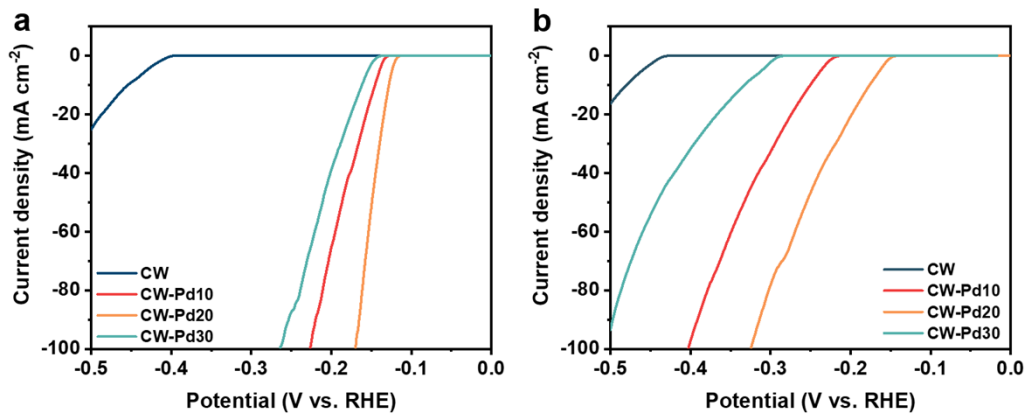


**Figure S4.** LSV curves of CW and CW-Pd with different ALD cycles in a) 0.5M  $\text{H}_2\text{SO}_4$ , b) 1M PBS ( $\text{pH} = 7.2$ )

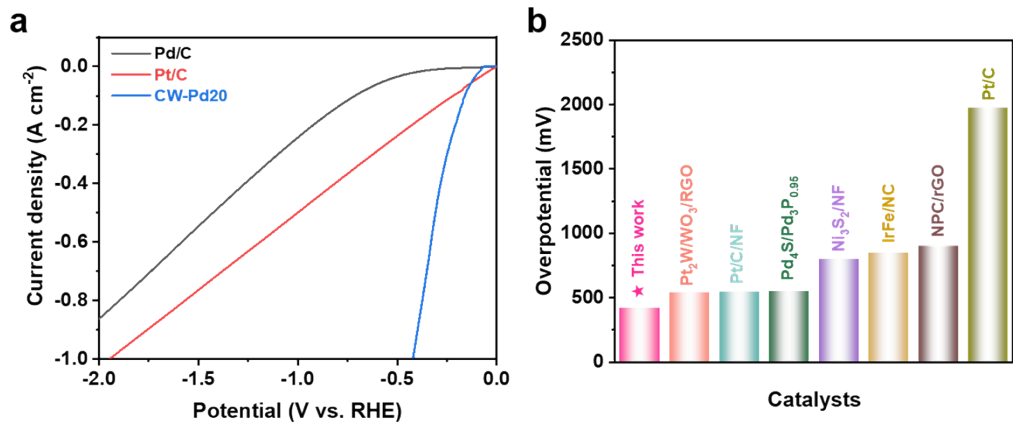


**Figure S5.** (a) LSV curves of CW-Pd20, commercial Pt/C and Pd/C in 1M KOH. (b) the comparison of overpotentials at  $1 \text{ A cm}^{-2}$  for CW-Pd20 and other reported electrocatalysts<sup>1-6</sup>.

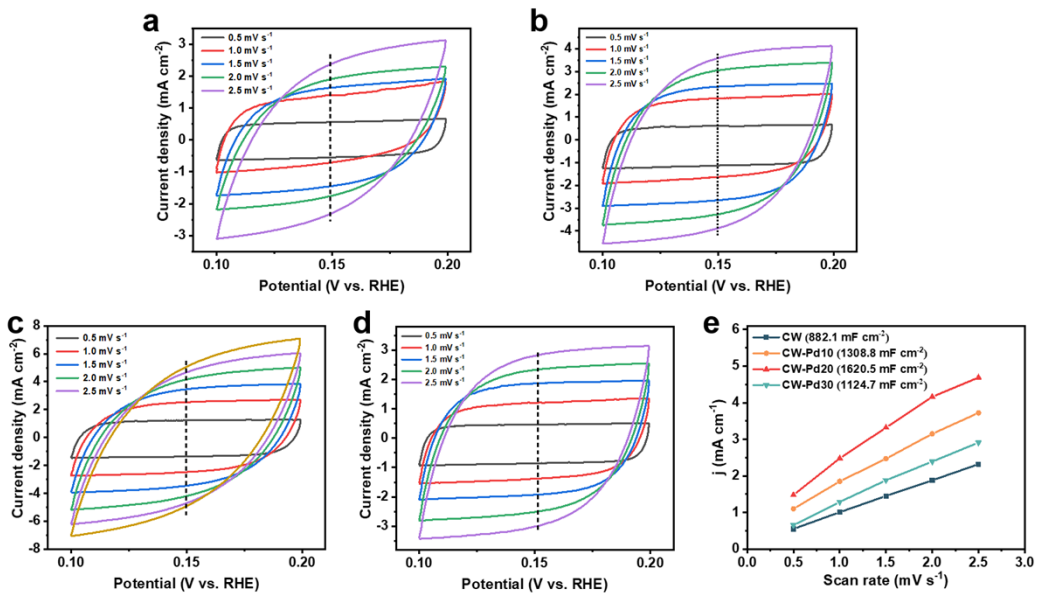


**Figure S6.** CV curves of a) CW, b) CW-Pd10, c) CW-Pd20, d) CW-Pd30. e) The electrochemical double-layer capacitance for CW and CW-Pd with different ALD cycles.

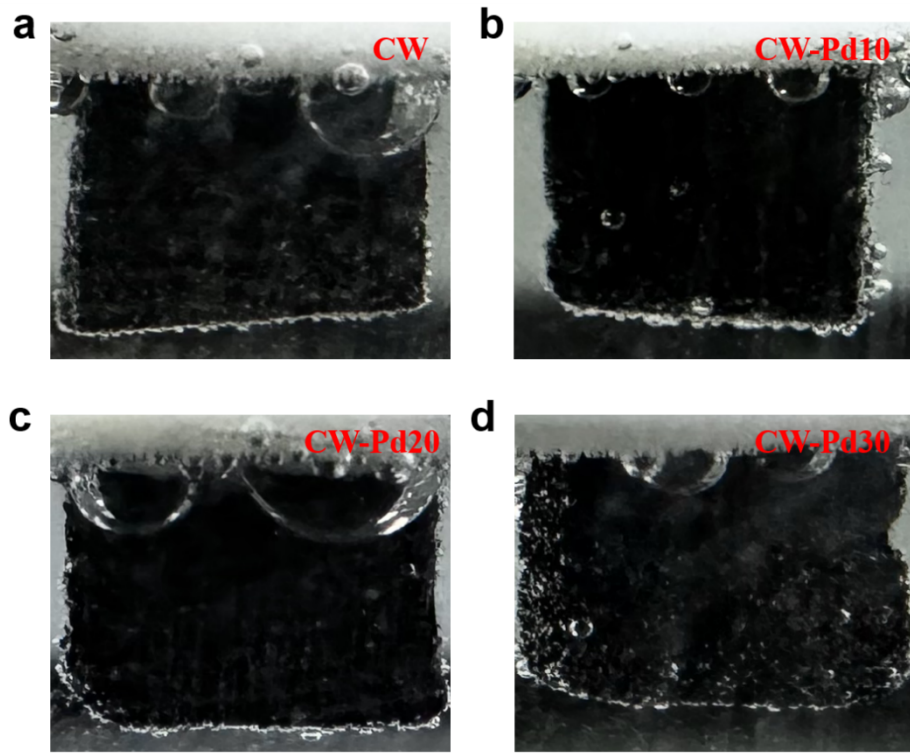


**Figure S7.** The optical figures of a) CW, b) CW-Pd10, c) CW-Pd20, d) CW-Pd30 during HER process.

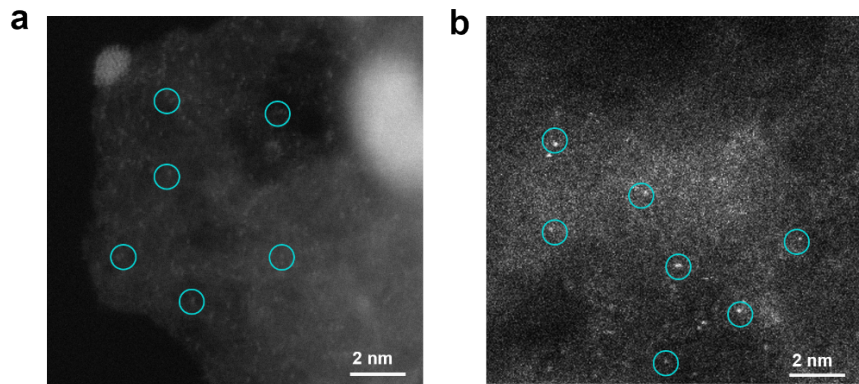


**Figure S8.** The HAADF-STEM images of CW-Pd20 (a) before and (b) after 40h stability test.

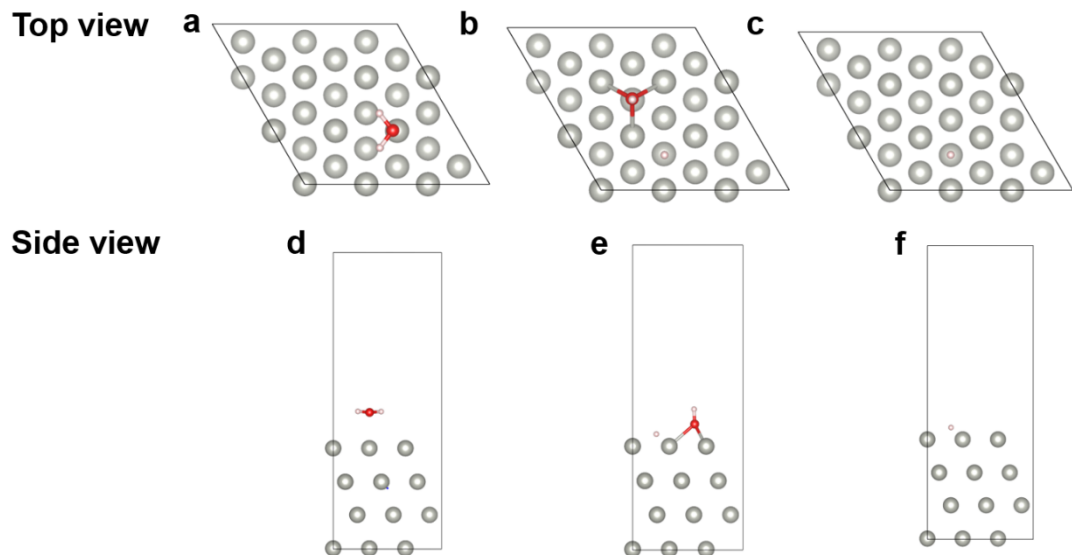


**Figure S9.** Optimized structure of a, d) H<sub>2</sub>O adsorbed, b, e) H<sub>2</sub>O dissociate, c, f) H adsorbed on Pd (111) containing 4 slabs with 12 Å vacuum layer.

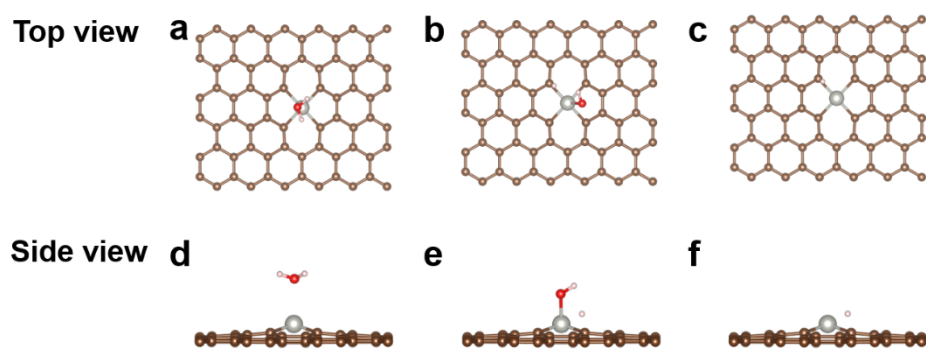


**Figure S10.** Optimized structure of a, d) H<sub>2</sub>O adsorbed, b, e) H<sub>2</sub>O dissociate, c, f) H adsorbed on Pd<sub>SA</sub> with 12 Å vacuum layer.

**Table S1.** The Raman fitting results of CW and CW-Pd.

	D1	D2	D3	D4	G	D1+D4
CW	46.9	0.9	20.0	12.8	19.4	59.7
CW-Pd10	48.0	1.7	19.7	11.4	19.2	59.4
CW-Pd20	46.9	0.9	20.0	12.8	19.4	59.7
CW-Pd30	46.2	0.6	18.8	13.7	20.7	59.9

**Table S2.** Elemental composition of the CW-Pd20 from XPS.

Catalyst	Pd (wt. %)	C (wt. %)	O (wt. %)
CW-Pd20	0.2	93.9	5.9

**Table S3.** Structure information of CW-Pd20 extracted from EXAFS fitting.

path	N	R	E <sub>0</sub>	sigma^2	R-factor
Pd-C/O	0.73±0.61	2.16±0.082	19.7±7.1	0.001	0.015
Pd-Pd	4.61±0.9	2.73±0.006	4.61±0.9	0.005	

## Reference

- Y. W. Peng, C. Shan, H. J. Wang, L. Y. Hong, S. Yao, R. J. Wu, Z. M. Zhang and T. B. Lu, *Advanced Energy Materials*, 2019, **9**, 1900597.
- G. Zhang, A. Wang, L. Niu, W. Gao, W. Hu, Z. Liu, R. Wang and J. Chen, *Advanced Energy Materials*, 2022, **12** 2103511.
- K. Sun, L. Zeng, S. Liu, L. Zhao, H. Zhu, J. Zhao, Z. Liu, D. Cao, Y. Hou, Y. Liu, Y. Pan and C. Liu, *Nano Energy*, 2019, **58**, 862-869.
- G. Li, J. Yu, J. Jia, L. Yang, L. Zhao, W. Zhou and H. Liu, *Advanced Functional Materials*, 2018, **28**, 1801332.
- W. He, R. Zhang, D. Cao, Y. Li, J. Zhang, Q. Hao, H. Liu, J. Zhao and H. L. Xin, *Small*, 2022, **19**, 2205719.

6. P. Jiang, H. Huang, J. Diao, S. Gong, S. Chen, J. Lu, C. Wang, Z. Sun, G. Xia, K. Yang, Y. Yang, L. Wei and Q. Chen, *Applied Catalysis B: Environmental*, 2019, **258**, 117965.